Atmospheric Environment 352 (2025) 121205

Contents lists available at ScienceDirect

Atmospheric Environment

journal homepage: www.elsevier.com/locate/atmosenv

Source attribution of near-surface ozone pollution in Jiangsu Province of China over 2013–2019

Siqi He [a,b], Yang Yang [a,b,*], Hailong Wang [c], Pinya Wang [a,b], Hong Liao [a,b]

[a] State Key Laboratory of Climate System Prediction and Risk Management, Jiangsu Key Laboratory of Atmospheric Environment Monitoring and Pollution Control, Jiangsu Collaborative Innovation Center of Atmospheric Environment and Equipment Technology, Joint International Research Laboratory of Climate and Environment Change, Nanjing University of Information Science and Technology, Nanjing, Jiangsu, China

[b] School of Environmental Science and Engineering, Nanjing University of Information Science and Technology, Nanjing, Jiangsu, China

[c] Atmospheric, Climate, and Earth Sciences Division, Pacific Northwest National Laboratory, Richland, WA, USA

HIGHLIGHTS

- Ozone in Jiangsu is mainly from remote NO_x emissions via long-range transport.
- Local anthropogenic NO_x emissions contribute 13 % to annual ozone in Jiangsu.
- Transportation and industry sectors are the main anthropogenic sources in Jiangsu.
- Extreme ozone pollution are due to both enhanced production and regional transport.

ABSTRACT

Near-surface ozone (O_3) is one of the most severe air pollutants in China, particularly over densely populated Jiangsu Province in the Yangtze River Delta. In this study, an O_3 source tagging technique is utilized in a chemistry-climate model to quantify the source contributions of various emission sectors and regions for nitrogen oxides (NO_x) and volatile organic compounds (VOCs) to O_3 concentrations in Jiangsu Province during 2013–2019. The results show that the near-surface O_3 in Jiangsu Province is mainly contributed by surrounding and remote anthropogenic NO_x emissions through long-range transport. Local anthropogenic NO_x emissions account for only 13 % and 18 % of the annual and summertime mean near-surface O_3 in Jiangsu Province, respectively. Anthropogenic NO_x emissions from the surface transportation, industry, and energy sectors account for 21 %, 22 % and 20 % of the annual mean near-surface O_3 concentration in Jiangsu Province, respectively. Biogenic and anthropogenic VOCs emissions each explains one-third of the annual mean near-surface O_3 concentration in Jiangsu, while methane and stratospheric chemical production contribute 21 % and 6 %, respectively. The sources from stratospheric production, aircraft, lightning, and foreign emissions are the primary contributors to O_3 in the mid- and high troposphere. During high pollution days in Jiangsu Province, the near-surface O_3 concentrations increase with the maximum exceeding 20 ppb, which is attributed to both the enhanced photochemical production and regional transport in favorable meteorological conditions.

1. Introduction

Ozone (O_3) in the troposphere is an important air pollutant with strong oxidizing properties (Voulgarakis et al., 2013; Turner et al., 2015; Lefohn et al., 2017; Lefohn et al., 2018). When the O_3 concentration reaches a certain level, it can damage human upper respiratory tract and lungs (Lim et al., 2012) and affect the production process of plants (Lefohn et al., 2018). O_3 near the surface is primarily generated by photochemical reactions between nitrogen oxides (NO_x) and volatile organic compounds (VOCs), through complex chemical mechanisms (Monks et al., 2015). It is also contributed by the stratosphere-troposphere exchange (Lelieveld et al., 2000; Chen et al., 2024) and long-distance transport (Li et al., 2002; Sudo and Akimoto, 2007; Pfister et al., 2013). Due to the relative long chemical life of tropospheric O_3 (Jacob et al., 1999; Bates and Jacob, 2020), the long-distance transport of O_3 brings great difficulty and uncertainty to the control of regional near-surface O_3 pollution (Stevenson et al., 2006; Wang et al., 2023). In addition to affecting human health, as a greenhouse gas (Stevenson et al., 2013; Myhre et al., 2013), O_3 also impacts the atmospheric radiation balance and global climate change (Szopa et al., 2021).

In recent decades, O_3 concentration in East Asia, especially China,

* Corresponding author. State Key Laboratory of Climate System Prediction and Risk Management, Jiangsu Key Laboratory of Atmospheric Environment Monitoring and Pollution Control, Jiangsu Collaborative Innovation Center of Atmospheric Environment and Equipment Technology, Joint International Research Laboratory of Climate and Environment Change, Nanjing University of Information Science and Technology, Nanjing, Jiangsu, China.

E-mail address: yang.yang@nuist.edu.cn (Y. Yang).

https://doi.org/10.1016/j.atmosenv.2025.121205
Received 3 December 2024; Received in revised form 8 March 2025; Accepted 27 March 2025
Available online 27 March 2025

shows a significant upward trend (Gaudel et al., 2018; Lin et al., 2017; Schultz et al., 2017). Since the 2010s, China's air pollution prevention and control has focused on $PM_{2.5}$ (particulate matter less than 2.5 μm in diameter). Through unremitting efforts, the problem of $PM_{2.5}$ pollution in China has been significantly alleviated (Chen et al., 2018; Li et al., 2019a). However, the concentration of near-surface O_3 has increased (Thomas et al., 2012; Li et al., 2019a, 2019b; Liu et al., 2019) and it becomes one of the most severe air pollutants in China, making it a top priority for scientific research and control strategies (L. Li et al., 2019). O_3 near the surface in China typically comes from both local photochemical formation and regional transport from upwind regions (Ge et al., 2021; Wang et al., 2021; Zheng et al., 2010). Several studies quantified the sources of O_3 over the Beijing-Tianjin-Hebei (BTH) and the Pearl River Delta (PRD) regions in China (Duan et al., 2008; Li et al., 2012; Shen et al., 2015). Wang et al. (2021) used the GEOS-Chem adjoint model to analyze the precursors contributing to surface O_3 in the BTH of China in June 2019 and found that BTH O_3 on heavily polluted days was sensitive to local emissions and precursors emitted from the provinces south of BTH. Wang et al. (2020) quantified the source contribution to ground-level O_3 in Beijing and Shanghai in August 2013 using the Community Multiscale Air Quality (CMAQ) model with a source-oriented SAPRC-11 photochemical mechanism. They found that near-surface O_3 in Beijing was mainly attributed to local emissions (51 %) and emissions from Hebei Province (31 %), while local emissions (53 %) and emissions from Zhejiang (19 %) and Jiangsu (14 %) Provinces were the main contributors to O_3 in Shanghai. Li et al. (2012) applied the Comprehensive Air quality Model with extensions (CAMx) with the Ozone Source Apportionment Technology (OSAT) extensions to quantify the regional source contributions to surface O_3 in the PRD region during high O_3 episode days in July and November of 2006. They revealed that, while the contribution from sources outside PRD dominated the mean O_3 conditions, elevated local sources within PRD are the causative factor for the high O_3 episodes, with local contributions increasing from about 30 % during non-episode days to about 50 % during high O_3 episode days in the autumn and up to about 70 % in the summer.

Some studies focused on source apportionment of O_3 over the Yangtze River Delta (YRD) (Li et al., 2016). Shu et al. (2020) conducted O_3 source attribution in different synoptic weather conditions over the YRD during 2013–2017 based on OSAT technique in a regional transport model. They reported that summertime surface O_3 was sensitive to the predominant synoptic patterns, which modulate the local chemistry and regional transport of O_3, with the transportation and industrial emissions being the primary sources. Li et al. (2020) also found that transportation and industrial sources dominated the non-background O_3 production in Nanjing of YRD, which were responsible for 52 % and 25 %, respectively, based on the source-oriented CMAQ model simulation during a regional O_3 pollution event that occurred in the YRD in summer 2020. Yao et al. (2023) investigated the airflow transport trajectory of O_3 by combining the O_3 observational records with a HYSPLIT (hybrid single-particle Lagrangian integrated trajectory) model and revealed that emissions of air pollutants from the Shandong Peninsula, the Korean Peninsula-Japan, and the Philippine Sea-Taiwan area aggravated O_3 pollution in the YRD region in summer from 2015 to 2021. These source apportionment studies used regional models that were mostly conducted for a single pollution event, and few study has examined the sources of O_3 from distant regions due to the domain limitation of regional models (Feng et al., 2016; Gao et al., 2016; Han et al., 2015; Li et al., 2017; Streets et al., 2007).

Source apportionment is a useful method to quantify the contribution of a specific source region or sector to air pollutants, which facilitates emission control strategies (Yang et al., 2018). Air mass trajectory tracking based on observations has been widely used to quantify the sources of air pollutants. However, the limitation of this method is that it assumes a constant lifetime of the contaminant and this method requires a large number of reverse cluster analysis of trajectories (Wang et al., 2006; Zheng et al., 2010; Liu et al., 2016a). Sensitivity analysis by perturbing emissions obtains the responses of O_3 concentrations to precursor emissions, providing information on the sensitivity of pollutants to changes in emissions (Fiore et al., 2009; Hoor et al., 2009), but it requires multiple simulations for individual emission perturbations. The source tagging method can provide information on the contribution of various emission sources to air pollutants and has been widely used in recent studies (Sudo and Akimoto, 2007; Zhang et al., 2008; Emmons et al., 2012; Grewe et al., 2017; Butler et al., 2018; Han et al., 2018; Batesand and Jacob, 2020; Butler et al., 2020). It considers the mass balance of air pollutants and does not have to concern the nonlinear relationship between concentration and emission. Perturbation methods are often used in the development of policies related to the amount of emission reductions with multiple simulations, while tagging methods can play a role in helping to determine which emissions to reduce in one single simulation (Butler et al., 2018).

Jiangsu Province, on the east coast of China, is a pivotal region in the Yangtze River Delta, which is one of China's most densely populated provinces, with a population exceeding 80 million. The region exhibits a humid subtropical climate, with significant seasonal variations in climate conditions (Xu et al., 2019). In recent years, Jiangsu has faced notable environmental challenges, particularly concerning air quality. Rapid industrialization and urbanization have contributed to elevated levels of air pollutants, including $PM_{2.5}$ and O_3. Despite efforts in mitigating pollution through various environmental policies and regulations, air quality issues persist in Jiangsu Province and the broader YRD region.

In view of this, by adopting an O_3 tagging technique in a global chemistry-climate model, the near-surface O_3 concentrations in Jiangsu Province in recent years (2013–2019) contributed from various emitting regions and sectors of O_3 precursors are systematically quantified. This study is the first to apply the tagging technique in global chemistry-climate modeling to the study of source attributions of near-surface O_3 in Jiangsu Province by tagging the O_3 precursors NO_x and VOCs separately. Sect. 2 describes the model description, tagging technique, emissions and observations, experimental design, and model evaluation. Sect. 3 quantifies contributions to O_3 in Jiangsu from different source regions and sectors. Sect. 4 summarizes the main conclusions and discusses this study. The contributions of anthropogenic emissions from different sectors, local emissions, long-distance transport, and stratosphere-troposphere exchange to the local O_3 pollution are explored to demonstrate the importance of regional coordination of prevention and control strategies and provide references for air quality management in Jiangsu Province. The meteorological influences and causes of the occurrence of high O_3 pollution days are also discussed to provide directions for early warning of severe pollution events.

2. Method

2.1. Model description

The Community Atmosphere Model version 4 with chemistry (CAM4-chem) (Lamarque et al., 2012; Tilmes et al., 2015), which is the atmospheric chemistry component of the Community Earth System Model (CESM), is utilized to simulate tropospheric O_3 concentration. The spatial resolution of the atmospheric model is 1.9° (latitude) × 2.5° (longitude) with 26 vertical layers. The model configuration uses a tropospheric chemistry mechanism based on the Model for Ozone and Related chemical Tracers version 4 (MOZART-4) (Emmons et al., 2010, 2012). The wind fields are nudged towards the MERRA-2 (Modern Era Retrospective-Analysis for Research and Applications Version 2) reanalysis (Gelaro et al., 2017) to better constrain large-scale circulations by observations. The CAM4-chem performance in simulating tropospheric O_3 and precursors has been fully evaluated by Tilmes et al. (2015).

2.2. Ozone source tagging technique

The ozone source tagging technique designed for CAM4-chem was developed by Butler et al. (2018), which provides a separate attribution of tropospheric O_3 to emissions of its precursors from individual sources. It requires two individual simulations attributing O_3 to NO_x or VOCs. Details of the O_3 tagging technique are described in Butler et al. (2018). The tagging scheme is different from the schemes in the regional models, such as CMAQ-ISAM and CAMx OSAT, using threshold conditions to determine whether O_3 formation is NO_x- or VOCs-limited and then attribute the generation of O_3 to the tag carried by a certain precursor (VOCs or NO_x) (Dunker et al., 2002; Kwok et al., 2015). The tagging method used in this study attributes O_3 production to both NO_x and VOCs and do not use the chemical indicators (Lupaşcu and Butler, 2019; Mertens et al., 2020).

In this study, near-surface O_3 is attributed to emitting sectors and regions. NO_x and VOCs are separately tagged in two parallel simulations. For the regional sources, we separate the global sources of anthropogenic emissions into nine regions, including Northwestern China (NWC), Himalayas and Tibetan Plateau (HTP), Central China (CTC), Northeastern China (NEC), North China Plain (NCP), Eastern China excluding Jiangsu Province (ECE), Jiangsu Province (JSP), Southern China (STC), and the rest of the World (ROW) (Fig. 1). For the emitting sectors, anthropogenic emissions from agriculture (AGR), energy (ENE), industry (IND), residential, commercial and other (RCO), surface transportation (TRA), solvent production and application (SLV), waste management (WST), international shipping (SHP) are separated tagged. Biomass burning emissions (BMB), biogenic emissions (BIO), soil emissions (SOL), lightning production (LGT), aircraft emissions (AIR), chemical production in the stratosphere (STR), extra chemical production (XTR), methane produced (CH_4) and carbon monoxide produced (CO) are also tagged in simulations if they exist.

2.3. Emissions and observations

The global anthropogenic emissions, including NO_x, non-methane VOCs (NMVOCs) and CO over 2010–2019 are from the Community Emissions Data System (CEDS) version 20210205 (Hoesly et al., 2018). Biomass burning emissions are derived from CMIP6 (Coupled Model Intercomparison Project Phase 6) over 2010–2014 (van Marle et al., 2017) and the remaining years (2015–2019) are obtained from SSP2-4.5 forcing scenario (O'Neill et al., 2016), because CMIP6 historical data do not include biomass burning emissions over 2015–2019. Soil NO_x emissions and biogenic NMVOCs emissions, as specified in Tilmes et al. (2015), are kept at the present-day (2000) climatological levels during simulations. Lightning emissions of NO_x are estimated according to Price et al. (1997). CH_4 concentration is kept constant at present-day level during simulations. To evaluate model performance, hourly O_3 concentrations obtained from the China National Environmental Monitoring Centre (CNEMC) (https://air.cnemc.cn:18007) are utilized for validation against simulated results.

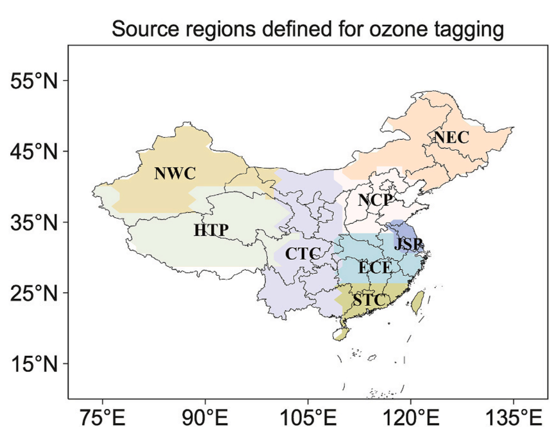

Fig. 1. Source regions defined for O_3 tagging, including Northwestern China (NWC), Himalayas and Tibetan Plateau (HTP), Central China (CTC), Northeastern China (NEC), North China Plain (NCP), Eastern China excluding Jiangsu Province (ECE), Jiangsu Province (JSP), Southern China (STC), and the rest of the World (ROW).

2.4. Experimental design

Four groups of experiments are conducted in this study. Each group includes both a NO_x-tagging simulation and a VOCs-tagging simulation. Two BASE experiment groups are carried out with tagging emission sectors and regions, respectively, driven by time-varying anthropogenic emissions and MERRA-2 reanalysis during 2010–2019. Two remaining sensitivity experiment groups are the same as BASE, except that anthropogenic emissions are fixed at 2019 during simulations, which aim to investigate the role of the meteorological fields in the O_3 differences between high pollution days and the normal days. The first 3 years are considered as model spin-up and the last 7 years are used for analyses. Unless otherwise stated, the BASE experiments are analyzed to quantify source attribution of O_3 in Jiangsu Province of China.

2.5. Model evaluation

Fig. 2 compares the model-simulated mean O_3 concentrations during the warm (May–September) and cold (December-January-February) seasons averaged over 2013–2019 with the observed data for the same time period. In general, the model overestimates O_3 mixing ratios in China warm seasons by 35 % (Table S1), while underestimates NO_2 mixing ratios by 40 % (Table S2). The O_3 bias is partly related to the simplified dry deposition scheme in CAM4 (Val Martin et al., 2014) and the possible strong photochemical reaction converting NO_x to O_3. It can also be attributed to the coarse resolution of the model. The model can capture the seasonal pattern of O_3 with high mixing ratios in the warm season and low mixing ratios in the cold season. The spatial distributions can also be roughly simulated by the model, with statistically significant correlation coefficients between simulations and observations in the range of 0.42–0.52. As patterns in China, the model also overestimates O_3 concentrations in Jiangsu Province, which suggests that the contributions of regional and sectoral sources to near-surface O_3 in Jiangsu could be overestimated in the model, especially in the warm season. As the emission reductions, the model can capture that the decreases in annual contributions to O_3 from anthropogenic emissions and increases in contributions from natural emissions (Tables S3 and S4).

3. Results

3.1. Source apportionment of ozone from emitting regions

Fig. 3 shows the relative contributions of NO_x and VOCs emissions from individual source regions to seasonal and annual near-surface O_3 concentration in Jiangsu Province during the analyzed period and Tables S5 and S6 summarize the values. In the NO_x-tagging experiment, anthropogenic sources from the rest of the world (ROW), the rest of the eastern region (ECE), local emissions in Jiangsu Province (JSP) and North China Plain (NCP) are the top four contributors to annual mean near-surface O_3 concentration in Jiangsu Province, explaining 25 %, 19 %, 13 % and 13 % of the annual mean concentration. Anthropogenic NO_x emissions from ECE and JSP have the largest contributions in summer, when the photochemical reaction is intense, accounting for 28 % and 18 %, respectively, and the smallest contributions (both 5 %) in winter. The contribution of sources from ROW is the largest in winter, with a proportion of 34 %. The contribution of stratospheric chemical production (STR) to near-surface O_3 in Jiangsu Province is smallest in summer (1 %) and largest in winter (19 %) and the contributions of NO_x

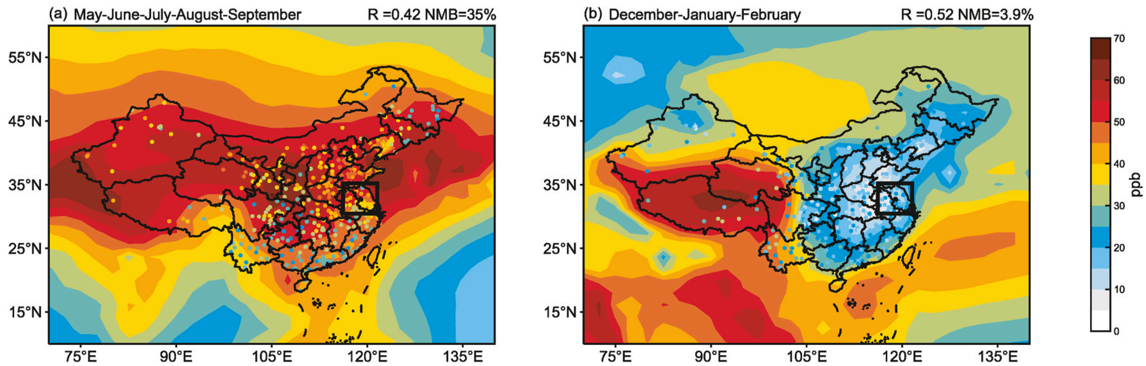

Fig. 2. The simulated (contours) and observed (scatters) mean near-surface O_3 concentrations (ppb) over the China during the (a) warm (May-June-July-August-September) and (b) cold (December-January-February) seasons averaged over 2013–2019. The correlation coefficient and normalized mean bias (NMB, Σ(Model −Observation)/Σ Observation × 100 %) are shown on the top right of each panel. The region of Jiangsu Province (30°45′–35°20′N,116°18′-121°57′E) is marked with black box.

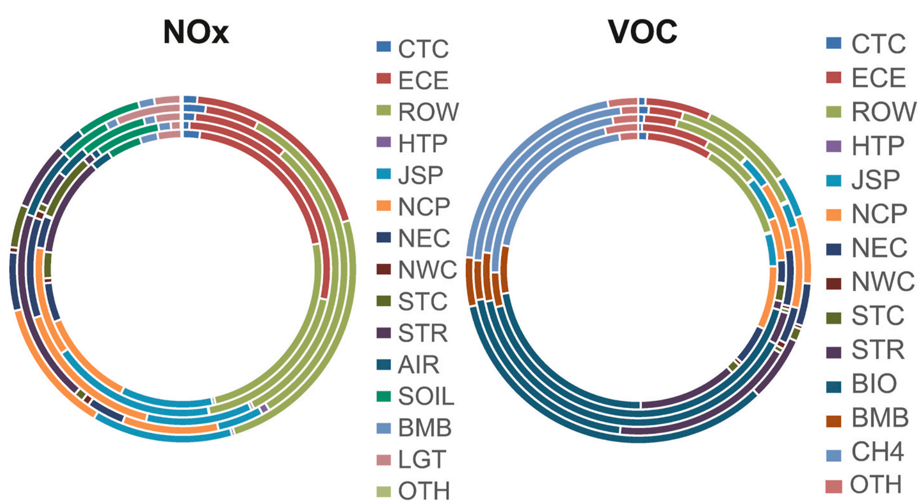

Fig. 3. Relative contributions (%) of NO_x and VOCs emissions from individual source regions to the seasonal and annual near-surface O_3 concentration in the tagged area in Jiangsu Province over 2013–2019. Circles from inner to outer illustrate the apportionment for spring (March-April-May), summer (June-July-August), autumn (September-October-November), winter (December-January-February) and annual average, respectively, in percentage relative to the respective total near-surface O_3 concentration. Sources with small contributions are combined and shown as OTH.

emitted from soil (SOIL) in summer and autumn are the largest (both 7 %) among the four seasons. It is revealed that, from the NO_x perspective, the near-surface O_3 in Jiangsu Province is primarily attributed to the surrounding and remote anthropogenic sources through long-range transport (44 %), while local emissions only account to 13 % of annual mean O_3 in Jiangsu.

In the VOCs-tagging experiment, biogenic VOCs emission (BIO), methane (CH_4), and ROW are the major sources of annual mean near-surface O_3 in Jiangsu Province, accounting for 34 %, 21 % and 9 %. Biogenic VOCs emissions account for a large proportion of contribution in all seasons, especially in summer (42 %). The contributions of CH_4 and ROW to near-surface O_3 in Jiangsu Province reach the maximum in winter, by 22 % and 14 %, respectively. STR contributes to 6 % of O_3 in Jiangsu Province annually, and the STR contribution reaches its peak in

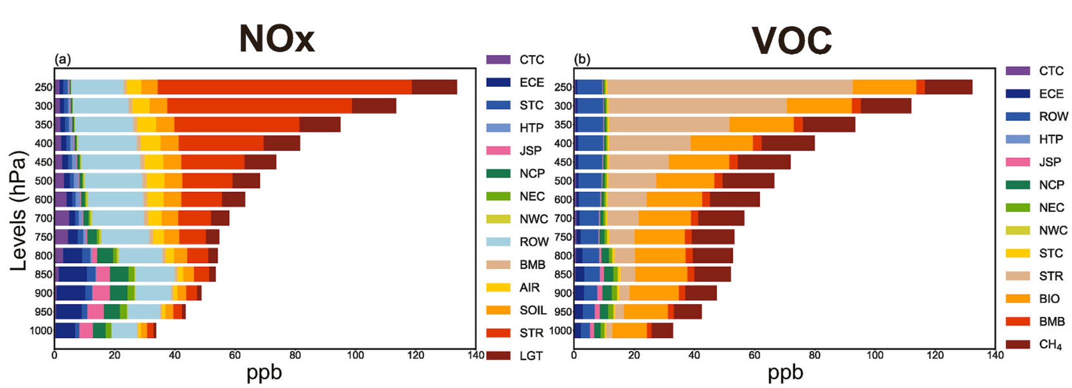

Fig. 4. Vertical profile of contributions (ppb) from individual source regions to annual mean O_3 concentrations in Jiangsu Province.

winter (18 %). The local anthropogenic VOCs emissions (JSP) have small contributions in all seasons (less than 5 %). It suggests that, from the perspective of VOCs, the near-surface O_3 in Jiangsu Province is mainly attributed to biogenic sources and CH_4 (55 %), while local emissions account for only 4 % of annual average O_3 in Jiangsu.

Fig. 4 presents the vertical profile of contributions from individual source regions to annual mean O_3 concentrations in Jiangsu Province. In the NO_x-tagging experiment, ECE and ROW emissions are the primary sources of O_3 in Jiangsu Province below 700 hPa. NCP and JSP local emissions also considerably contribute to O_3 at this level. O_3 from stratosphere and contributions from aircraft, lightning and ROW increase with height and become the major contributors of O_3 in Jiangsu Province above 700 hPa. In VOCs-tagging, biogenic VOCs and CH_4 together explain more than half of the O_3 in Jiangsu from the surface to 500 hPa, while the O_3 from stratosphere dominates the concentration at the upper troposphere.

3.2. Source apportionment of ozone from emitting sectors

Fig. 5 shows the relative contributions of NO_x and VOCs emissions from individual source sectors to seasonal and annual near-surface O_3 concentration in Jiangsu Province during the analyzed period and Tables S7 and S8 summarize the values. In the NO_x-tagging experiment, anthropogenic emissions from the surface transportation (TRA), industry (IND), and energy (ENE) sectors are the three primary contributors to the annual average near-surface O_3 concentration in Jiangsu Province, explaining 22 %, 21 %, and 20 % of the annual concentration, respectively. Natural NO_x emissions from soil (SOIL), stratospheric chemical production (STR), and lightning NO_x emissions (LGT) account for only 6 %, 6 % and 4 % of the annual mean concentration of surface O_3 in Jiangsu Province. It reveals that, from the NO_x perspective, the near-surface O_3 in Jiangsu Province are primarily attributed to anthropogenic sources (83 %), especially from ground transportation, industry and energy sectors, while natural sources only account for 17 % of annual O_3 in Jiangsu.

In the VOCs-tagging experiment, anthropogenic VOCs emissions account for 34 % of annual near-surface O_3 concentration in Jiangsu Province and this contribution reaches the maximum in spring (41 %). Surface transportation, industry, energy and residential sectors each contributes 6 %–8 % of the annual O_3 in Jiangsu. Consistent with the regional contribution analysis, biogenic VOCs are the major source sector of annual mean near-surface O_3 concentration in Jiangsu Province contributing about one-third of the O_3 concentration, followed by the contribution from CH_4.

Fig. 6 presents the vertical profile of contributions from individual source sectors to annual mean O_3 concentrations in Jiangsu Province. In the NO_x-tagging experiment, TRA, ENE and IND emissions are the primary anthropogenic sources of O_3 in Jiangsu Province below 800 hPa. The O_3 from stratosphere dominates the concentration at the upper troposphere. In the VOC-tagging experiment, the anthropogenic VOCs together explain less than one-third of the O_3 in Jiangsu from the surface to 500 hPa, while biogenic VOCs largely contribute O_3 throughout the troposphere.

3.3. Source apportionment of ozone during polluted days

Understanding the sources of O_3 on pollution days in Jiangsu Province can help to establish an effective and scientific way of reducing air pollution events. The O_3 pollution days are identified as the days when the daily O_3 in the receptor area (i.e. Jiangsu Province) is above the 90th percentile of the probability density of O_3 concentrations during May–September (Fig. S1), when the O_3 pollution is severe in China. In the 7-year simulation, in total 111 days are identified as polluted days in Jiangsu Province.

Fig. 7 shows the composite differences in near-surface O_3 concentrations and 850 hPa winds between O_3 pollution days and normal days in Jiangsu Province, and Fig. 8 presents the composite differences in the influencing meteorological factors. When Jiangsu Province is under the polluted condition, with near-surface O_3 concentrations higher than normal, the maximum increase in O_3 concentration exceeds 20 ppb (Fig. 7a). During the polluted days, the surface air temperature is higher than normal across China. Incoming solar radiation increases in Jiangsu Province and surrounding regions, while cloud fraction and relative humidity decrease over these regions. These changes in the meteorological factors favor the local chemical production of O_3, contributing to the high O_3 concentrations during the polluted days. In addition, during the O_3 pollution days, an anomalous cyclone is located over the northwestern Pacific and the associated anomalous northerly winds can transport O_3 from the polluted NCP to the south, partly explaining the O_3 increases in Jiangsu.

Fig. 9 summarizes the source contributions to the differences from individual emission source regions. During the O_3 pollution days in Jiangsu Province, local NO_x emissions and sources from surrounding ECE region contribute 4.5 ppb and 9.9 ppb to the O_3 concentration

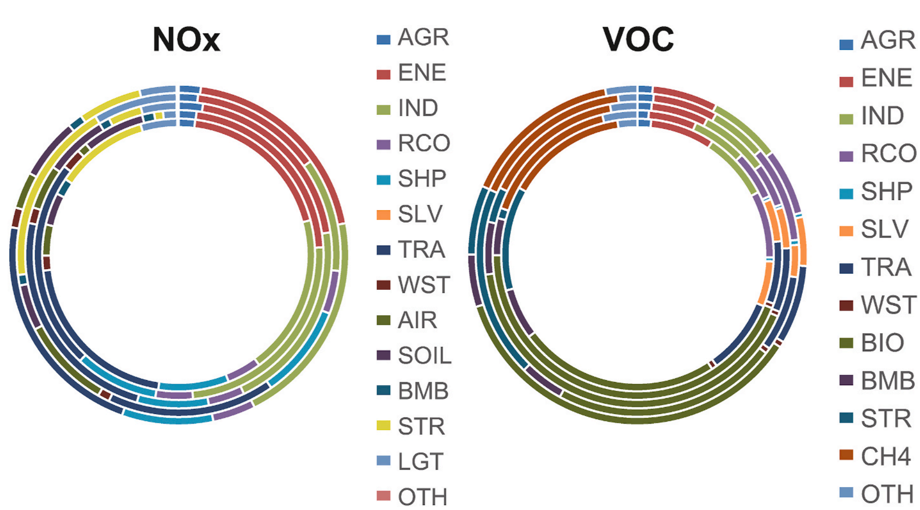

Fig. 5. Relative contributions (%) of NO_x and VOCs emissions from individual source sectors to the seasonal and annual near-surface O_3 concentration in the tagged area in Jiangsu Province over 2013–2019. Circles from inner to outer indicate spring (March-April-May), summer (June-July-August), autumn (September-October-November), winter (December-January-February) and annual average, respectively, in percentage relative to the total near-surface O_3 concentration. Sources with small contributions are combined and shown as OTH.

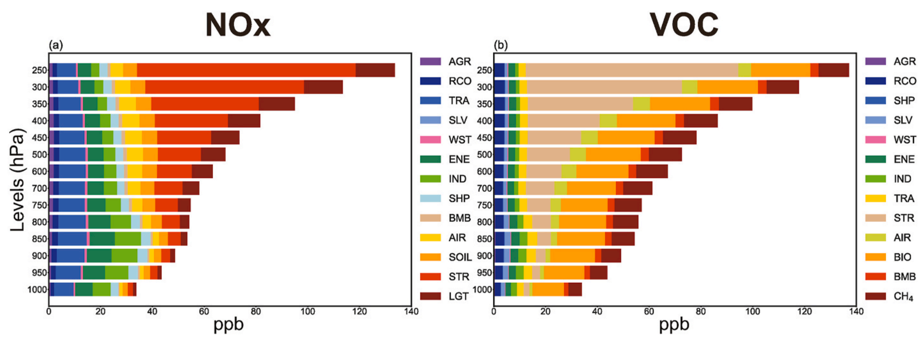

Fig. 6. Vertical profile of contributions (ppb) from individual sectors to annual mean O_3 concentrations in Jiangsu Province.

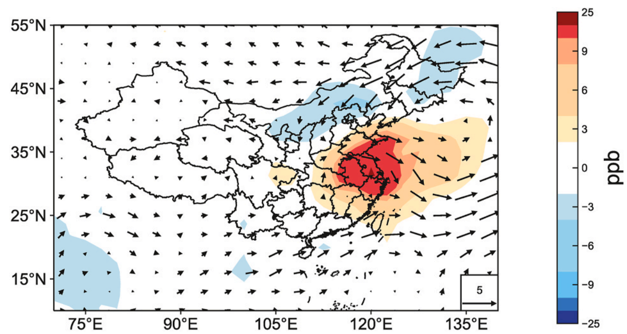

Fig. 7. Composite differences in near-surface O_3 concentrations (contours, ppb) and 850 hPa winds (vectors, m s^{-1}) between O_3 pollution days and normal days during May–September.

increase in Jiangsu Province, accounting for 85 % of the total increase, owing to the enhanced photochemical production in favorable meteorological conditions. The anomalous northerly winds transport polluted air from NCP and contribute 6.6 ppb (39 % relative to the total increase) to O_3 concentration increase in Jiangsu Province in the polluted days. In the VOC-tagging experiment, VOCs from ECE, NCP and Jiangsu local sources are also the top three anthropogenic contributors to the O_3 increase in Jiangsu Province. It suggests that during the O_3 pollution days, the increase in near-surface O_3 concentration in Jiangsu Province is attributed to both the enhanced photochemical production and the regional transport. The source sectors analysis also shows that the NO_x contributions increase from the industry and energy sectors during the polluted days compared to the normal days, while the shipping contribution decreases (Tables S9 and S10), consistent with the decrease in ROW contribution (Fig. 9).

4. Conclusions and discussions

Jiangsu, a pivotal region in the Yangtze River Delta, which is one of China's most densely populated provinces, faces severe O_3 pollution in recent years. In this study, the source apportionment of near-surface O_3 from various emission source regions and sectors of O_3 precursors in Jiangsu Province is quantified using a global chemistry-climate model equipped with an O_3 source tagging technique.

The annual near-surface O_3 concentrations in Jiangsu Province are primarily contributed by surrounding and remote anthropogenic NO_x emissions through long-range transport, while local anthropogenic NO_x emissions account for only 13 % of the annual mean near-surface O_3. Anthropogenic NO_x emissions from ECE and Jiangsu have the largest contributions in summer, while ROW contributes significantly in winter. NO_x emissions from surface transportation, industry, and energy sectors account for 21 %, 22 % and 20 % of the annual mean O_3 concentration in Jiangsu Province, respectively. The source regions contributing to O_3 concentrations below 700 hPa are consistent with those for near-surface O_3, while stratosphere, aircraft, lightning, and ROW are the primary contributors to O_3 above 700 hPa. Anthropogenic and biogenic VOCs emissions each account for one-third of the annual mean near-surface O_3 concentration in Jiangsu Province, while CH_4 and stratospheric chemical production contribute 21 % and 6 %, respectively. Biogenic VOCs

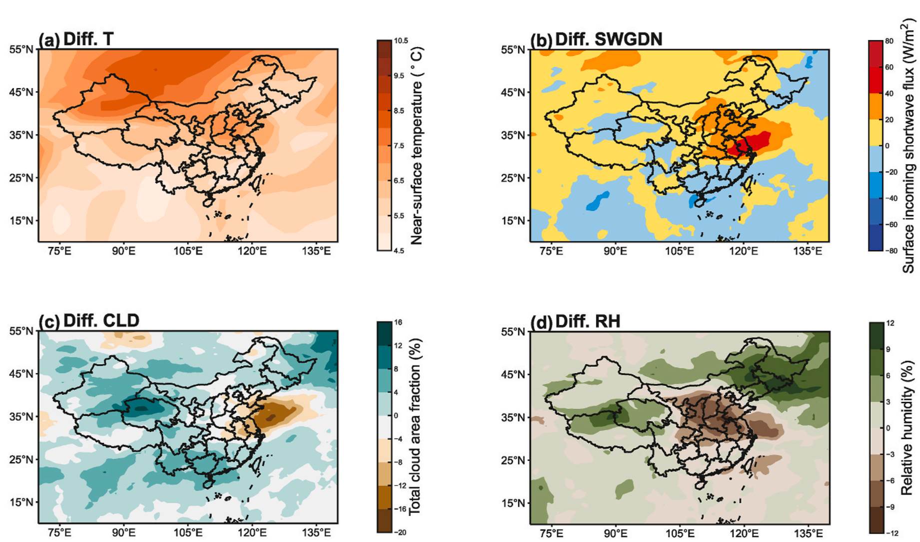

Fig. 8. Composite differences in (a) surface air temperature (°C), (b) surface incoming shortwave flux (W m^{-2}), (c) cloud fraction (%), and (d) relative humidity (%) between O_3 polluted days and normal days during May–September.

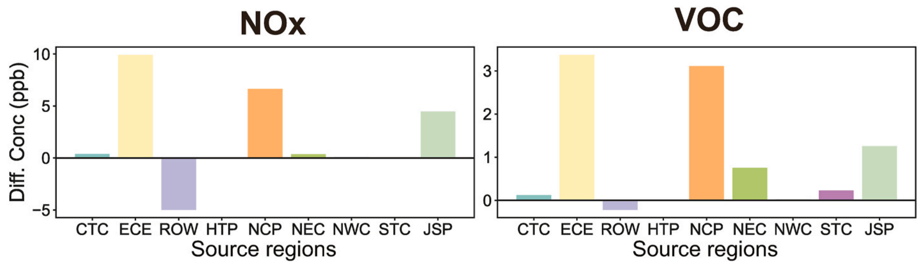

Fig. 9. Contributions (ppb) of anthropogenic NO_x (left) and VOCs (right) emissions from individual source regions to the increase in near-surface O_3 concentration in Jiangsu Province between O_3 polluted days and normal days during May–September.

emissions account for a large portion of contribution in all seasons, especially in summer. The contribution of biogenic VOCs is the largest in summer, while the contribution of CH_4 reaches the maximum in winter.

During the O_3 pollution days, the near-surface O_3 concentration in Jiangsu Province increases by a maximum of 20 ppb, which is attributed to both the enhanced photochemical production and the regional transport. Changes in meteorological factors such as higher temperatures, increased incoming solar radiation, and decreases in cloud fraction and relative humidity over Jiangsu and surrounding regions are conducive to the chemical formation of O_3, resulting in an increase in O_3 concentration during the polluted days. In addition, an anomalous cyclone is located over the northwestern Pacific and the associated anomalous northerly winds transport polluted air from NCP, which contributes 39 % to the O_3 concentration increase in Jiangsu Province in the polluted days.

In this study, the dominance of transboundary contributions from surrounding regions and remote areas highlights the necessity of coordinated emission controls across the Yangtze River Delta and adjacent provinces and the need to strengthen international cooperation. Regional joint action plans targeting anthropogenic NO_x emissions from industry, energy, and transportation sectors should be prioritized. With biogenic and anthropogenic VOCs each contributing about one third to annual O_3 levels, policies should balance reductions in anthropogenic VOCs (e.g., solvents, petrochemicals) with strategies to mitigate biogenic VOCs impacts through urban greening optimization (e.g., selecting low-emission tree species).

It should be noted that the model overestimates the regional O_3 concentration in China, partly due to the coarse model resolution and possible deficiency in the O_3 chemistry of the model. The model setup of fixing soil NO_x emissions and biogenic emissions at the current level could lead to the biases in the modeled interannual variability of natural contributions to O_3. In addition, only the wind fields are nudged towards the MERRA-2 reanalysis, without considering temperature and humidity nudging. These uncertainties may affect the quantitative results in this study, which should be revisited in future studies using improved state-of-the-science chemistry-climate models. Nevertheless, this study not only reveals the main drivers of near-surface O_3 in Jiangsu Province, but also provides an important reference for the development of cross-regional synergistic control strategies, which is particularly practically important in addressing intercontinental transport and intersectoral synergistic emission reduction.

CRediT authorship contribution statement

Siqi He: Writing – original draft, Visualization, Software, Methodology, Investigation, Formal analysis, Data curation, Conceptualization. **Yang Yang:** Writing – review & editing, Supervision, Project administration, Formal analysis, Data curation, Conceptualization. **Hailong Wang:** Writing – review & editing. **Pinya Wang:** Writing – review & editing. **Hong Liao:** Writing – review & editing.

Declaration of competing interest

The authors declare that they have no known competing financial interests or personal relationships that could have appeared to influence the work reported in this paper.

Acknowledgments

This study was supported by the National Natural Science Foundation of China (grants 42293320, 42475032), the National Key Research and Development Program of China (grant 2020YFA0607803) and Jiangsu Innovation and Entrepreneurship Team (grant JSSCTD202346). The Pacific Northwest National Laboratory (PNNL) is operated for DOE by the Battelle Memorial Institute under contract DE-AC05-76RLO1830.

Appendix A. Supplementary data

Supplementary data to this article can be found online at https://doi.org/10.1016/j.atmosenv.2025.121205.

Data availability

Data will be made available on request.

References

Bates, K.H., Jacob, D.J., 2020. An expanded definition of the odd oxygen family for tropospheric ozone budgets: implications for ozone lifetime and stratospheric influence. Geophys. Res. Lett. 47, e2019GL084486. https://doi.org/10.1029/2019gl084486.

Butler, T., Lupascu, A., Nalam, A., 2020. Attribution of ground-level ozone to anthropogenic and natural sources of nitrogen oxides and reactive carbon in a global chemical transport model. Atmos. Chem. Phys. 20, 10707–10731. https://doi.org/10.5194/acp-20-10707-2020.

Butler, T., Lupascu, A., Coates, J., Zhu, S., 2018. TOAST1.0: tropospheric ozone attribution of sources with tagging for CESM 1.2.2. Geosci. Model Dev. (GMD) 11, 2825–2840. https://doi.org/10.5194/gmd-11-2825-2018.

Chen, X., Wang, Z., Li, J., Yang, W., Chen, H., Wang, Z., Hao, J., Ge, B., Wang, D., Huang, H., 2018. Simulation on different response characteristics of aerosol particle number concentration and mass concentration to emission changes over mainland China. Sci. Total Environ. 643, 692–703. https://doi.org/10.1016/j.scitotenv.2018.06.181.

Chen, Z., Liu, J., Qie, X., Cheng, X., Yang, M., S, L., Z, Z., 2024. Stratospheric influence on surface ozone pollution in China. Nat. Commun. 15, 4064. https://doi.org/10.1038/s41467-024-48406-x.

Duan, J., Tan, J., Liu, Y., Shan, W., Hao, J., 2008. Concentration, sources and ozone formation potential of volatile organic compounds (VOCs) during ozone episode in Beijing. Atmos. Res. 88, 25–35. https://doi.org/10.1016/j.atmosres.2007.09.004.

Dunker, A.M., Yarwood, G., Ortmann, J.P., Wilson, G.M., 2002. Comparison of source apportionment and source sensitivity of ozone in a three-dimensional air quality model. Environ. Sci. Technol. 36, 2953–2964. https://doi.org/10.1021/es011418f.

Emmons, L.K., Hess, P.G., Lamarque, J.-F., Pfister, G.G., 2012. Tagged ozone mechanism for MOZART-4, CAM-chem and other chemical transport models. Geosci. Model Dev. (GMD) 5, 1531–1542. https://doi.org/10.5194/gmd-5-1531-2012.

Emmons, L.K., Walters, S., Hess, P.G., Lamarque, J.-F., Pfister, G.G., Fillmore, D., Granier, C., Guenther, A., Kinnison, D., Laepple, T., Orlando, J., Tie, X., Tyndall, G., Wiedinmyer, C., Baughcum, S.L., Kloster, S., 2010. Description and evaluation of the model for ozone and related chemical Tracers, version 4 (MOZART-4). Geosci. Model Dev. (GMD) 3, 43–67. https://doi.org/10.5194/gmd-3-43-2010.

Feng, T., Bei, N., Huang, R.-J., Cao, J., Zhang, Q., Zhou, W., Tie, X., Liu, S., Zhang, T., Su, X., Lei, W., Molina, L.T., Li, G., 2016. Summertime ozone formation in Xi'an and surrounding areas, China. Atmos. Chem. Phys. 16, 4323–4342. https://doi.org/10.5194/acp-16-4323-2016.

Fiore, A.M., Dentener, F.J., Wild, O., Cuvelier, C., Schultz, M.G., Hess, P., Textor, C., Schulz, M., Doherty, R.M., Horowitz, L.W., MacKenzie, I.A., Sanderson, M.G., Shindell, D.T., Stevenson, D.S., Szopa, S., van Dingenen, R., Zeng, G., Atherton, C., Bergmann, D., Bey, I., Carmichael, G., Collins, W.J., Duncan, B.N., Faluvegi, G., Folberth, G., Gauss, M., Gong, S., Hauglustaine, D., Holloway, T., Isaksen, I.S.A., Jacob, D.J., Jonson, J.E., Kaminski, J.W., Keating, T.J., Lupu, A., Marmer, E., Montanaro, V., Park, R.J., Pitari, G., Pringle, K.J., Pyle, J.A., Schroeder, S., Vivanco, M.G., Wind, P., Wojcik, G., Wu, S., Zuber, A., 2009. Multimodel estimates of intercontinental sourcereceptor relationships for ozone pollution. J. Geophys. Res. 114, D04301. https://doi.org/10.1029/2008JD010816.

Gao, J., Zhu, B., Xiao, H., Kang, H., Hou, X., Shao, P., 2016. A case study of surface ozone source apportionment during a high concentration episode, under frequent shifting wind conditions over the Yangtze River Delta, China. Sci. Total Environ. 544, 853–863. https://doi.org/10.1016/j.scitotenv.2015.12.039.

Gaudel, A., Cooper, O.R., Ancellet, G., Barret, B., Boynard, A., Burrows, J.P., Clerbaux, C., Coheur, P.-F., Cuesta, J., Cuevas, E., Doniki, S., Dufour, G., Ebojie, G., Foret, G., Garcia, O., Granados-Muñoz, M.J., Hannigan, J.W., Hase, F., Hassler, B., Huang, G., Hurtmans, D., Jaffe, D., Jones, N., Kalabokas, P., Kerridge, B., Kulawik, S., Latter, B., Leblanc, Le Flochmoën, E., Lin, W., Liu, J., Liu, X., Mahieu, E., McClure-Begley, A., Neu, J.L., Osman, M., Palm, M., Petetin, H., Petropavlovskikh, I., Querel, R., Rahpoe, N., Rozanov, A., Schultz, M.G., Schwab, J., Siddans, R., Smale, D., Steinbacher, M., Tanimoto, H., Tarasick, D.W., Thouret, V., Thompson, A.M., Trickl, T., Weatherhead, E., Wespes, C., Worden, H.M., Vigouroux, C., Xu, X., Zeng, G., Ziemke, J., 2018. Tropospheric Ozone Assessment Report: present-day distribution and trends of tropospheric ozone relevant to climate and global atmospheric chemistry model evaluation. Elem. Sci. Anth. 6, 39. https://doi.org/10.1525/elementa.291.

Gelaro, R., McCarty, W., Suárez, M.J., Todling, R., Molod, A., Takacs, L., Randles, C.A., Darmenov, A., Bosilovich, M.G., Reichle, R., Wargan, K., Coy, L., Cullather, R., Draper, C., Akella, S., Buchard, V., Conaty, A., da Silva, A.M., Gu, W., Kim, G., Koster, R., Lucchesi, R., Merkova, D., Nielsen, J.E., Partyka, G., Pawson, S., Putman, W., Rienecker, M., Schubert, S.D., Sienkiewicz, M., Zhao, B., 2017. The modern-Era Retrospective analysis for research and applications, version 2 (MERRA-2). J. Climate 30, 5419–5454. https://doi.org/10.1175/JCLI-D-16-0758.1.

Ge, S., Wang, S., Xu, Q., Ho, T., 2021. Source apportionment simulations of ground-level ozone in Southeast Texas employing OSAT/APCA in CAMx. Atmos. Environ. 253, 118370. https://doi.org/10.1016/j.atmosenv.2021.118370.

Grewe, V., Tsati, E., Mertens, M., Frömming, C., Jöckel, P., 2017. Contribution of emissions to concentrations: the TAGGING 1.0 submodel based on the modular Earth submodel System (MESSy 2.52). Geosci. Model Dev. (GMD) 10, 2615–2633. https://doi.org/10.5194/gmd-10-2615-2017.

Han, H., Liu, J., Yuan, H., Zhuang, B., Zhu, Y., Wu, Y., Yan, Y., Ding, A., 2018. Characteristics of intercontinental transport of tropospheric ozone from Africa to Asia. Atmos. Chem. Phys. 18, 4251–4276. https://doi.org/10.5194/acp-18-4251-2018.

Han, M., Lu, X., Zhao, C., Ran, L., Han, S., 2015. Characterization and source apportionment of volatile organic compounds in urban and suburban tianjin, China. Adv. Atmos. Sci. 32, 439–444. https://doi.org/10.1007/s00376-014-4077-4.

Hoesly, R.M., Smith, S.J., Feng, L., Klimont, Z., JanssensMaenhout, G., Pitkanen, T., Seibert, J.J., Vu, L., Andres, R.J., Bolt, R.M., Bond, T.C., Dawidowski, L., Kholod, N., Kurokawa, J.-I., Li, M., Liu, L., Lu, Z., Moura, M.C.P., O'Rourke, P.R., Zhang, Q., 2018. Historical (1750–2014) anthropogenic emissions of reactive gases and aerosols from the Community Emissions Data System (CEDS). Geosci. Model Dev. (GMD) 11, 369–408. https://doi.org/10.5194/gmd-11-369-2018.

Hoor, P., Borken-Kleefeld, J., Caro, D., Dessens, O., Endresen, O., Gauss, M., Grewe, V., Hauglustaine, D., Isaksen, I.S.A., Jöckel, P., Lelieveld, J., Myhre, G., Meijer, E., Olivie, D., Prather, M., Schnadt Poberaj, C., Shine, K.P., Staehelin, J., Tang, Q., van Aardenne, J., van Velthoven, P., Sausen, R., 2009. The impact of traffic emissions on atmospheric ozone and OH: results from QUANTIFY. Atmos. Chem. Phys. 9, 3113–3136. https://doi.org/10.5194/acp-9-3113-2009.

Jacob, D.J., Logan, J.A., Murti, P.P., 1999. Effect of rising Asian emissions on surface ozone in the United States. Geophys. Res. Lett. 26, 2175–2178. https://doi.org/10.1029/1999GL900450.

Kwok, R.H.F., Baker, K.R., Napelenok, S.L., Tonnesen, G.S., 2015. Photochemical grid model implementation and application of VOC, NOx, and O3 source apportionment. Geosci. Model Dev. (GMD) 8, 99–114. https://doi.org/10.5194/gmd-8-99-2015.

Lamarque, J.-F., Emmons, L.K., Hess, P.G., Kinnison, D.E., Tilmes, S., Vitt, F., Heald, C.L., Holland, E.A., Lauritzen, P.H., Neu, J., Orlando, J.J., Rasch, P.J., Tyndall, G.K., 2012. CAM-chem: description and evaluation of interactive atmospheric chemistry in the Community Earth System Model. Geosci. Model Dev. (GMD) 5, 369–411. https://doi.org/10.5194/gmd-5-369-2012.

Lelieveld, J., Dentener, F.J., 2000. What controls tropospheric ozone? J. Geophys. Res. 105, 3531–3551. https://doi.org/10.1029/1999jd901011.

Li, G., Bei, N., Cao, J., Wu, J., Long, X., Feng, T., Dai, W., Liu, S., Zhang, Q., Tie, X., 2017. Widespread and persistent ozone pollution in eastern China during the non-winter season of 2015: observations and source attributions. Atmos. Chem. Phys. 17, 2759–2774. https://doi.org/10.5194/acp-17-2759-2017.

Li, K., Jacob, D.J., Liao, H., Shen, L., Zhang, Q., Bates, K., 2019a. Anthropogenic drivers of 2013–2017 trends in summer surface ozone in China. P. Natl. Acad. Sci. USA 116, 422–427. https://doi.org/10.1073/pnas.1812168116.

Li, K., Jacob, D.J., Liao, H., Zhu, J., Shah, V., Shen, L., Bates, K., Zhang, Q., Zhai, S., 2019b. A two-pollutant strategy for improving ozone and particulate air quality in China. Nat. Geosci. 12, 906–910. https://doi.org/10.1038/s41561-019-0464-x.

Li, L., An, J., Huang, L., Yan, R., Huang, C., Yarwood, G., 2019. Ozone source apportionment over the Yangtze River Delta region, China: investigation of regional transport, sectoral contributions and seasonal differences. Atmos. Environ. 202, 269–280. https://doi.org/10.1016/j.atmosenv.2019.01.028.

Li, L., An, J., Shi, Y., Zhou, M., Yan, R., Huang, C., Wang, H., Lou, S., Wang, Q., Lu, Q., Wu, J., 2016. Source apportionment of surface ozone in the Yangtze River Delta, China in the summer of 2013. Atmos. Environ. 144, 194–207. https://doi.org/10.1016/j.atmosenv.2016.08.076.

Li, Q., 2002. Transatlantic transport of pollution and its effects on surface ozone in Europe and North America. J. Geophys. Res. 107, 4166. https://doi.org/10.1029/2001JD001422.

Li, Y., Lau, K.-H., Fung, C.-H., Zheng, J.Y., Zhong, L.J., Louie, P.K.K., 2012. Ozone source apportionment (OSAT) to differentiate local regional and super-regional source contributions in the pearl river delta region, China. J. Geophys. Res. 117, D15305. https://doi.org/10.1029/2011JD017340.

Lim, S.S., Vos, T., Flaxman, A.D., Danaei, G., Shibuya, K., Adair-Rohani, H., Amann, M., Anderson, H.R., Andrews, K.G., Aryee, M., Atkinson, C., Bacchus, L.J., Bahalim, A.N., Balakrishnan, K., Balmes, J., Barker-Collo, S., Baxter, A., Bell, M.L., Blore, J.D., Blyth, F., Bonner, C., Borges, G., Bourne, R., Boussinesq, M., Brauer, M., Brooks, P., Bruce, N.G., Brunekreef, B., Bryan-Hancock, C., Bucello, C., Buchbinder, R., Bull, F., Burnett, R.T., Byers, T.E., Calabria, B., Carapetis, J., Carnahan, E., Chafe, Z., Charlson, F., Chen, H.L., Chen, J.S., Cheng, A.T.A., Child, J.C., Cohen, A., Colson, K. E., Cowie, B.C., Darby, S., Darling, S., Davis, A., Degenhardt, L., Dentener, F., Des Jarlais, D.C., Devries, K., Dherani, M., Ding, E.L., Dorsey, E.R., Driscoll, T., Edmond, K., Ali, S.E., Engell, R.E., Erwin, P.J., Fahimi, S., Falder, G., Farzadfar, F., Ferrari, A., Finucane, M.M., Flaxman, S., Fowkes, F.G.R., Freedman, G., Freeman, M. K., Gakidou, E., Ghosh, S., Giovannucci, E., Gmel, G., Graham, K., Grainger, R., Grant, B., Gunnell, D., Gutierrez, H.R., Hall, W., Hoek, H.W., Hogan, A., Hosgood, H. D., Hoy, D., Hu, H., Hubbell, B.J., Hutchings, S.J., Ibeanusi, S.E., Jacklyn, G.L., Jasrasaria, R., Jonas, J.B., Kan, H.D., Kanis, J.A., Kassebaum, N., Kawakami, N., Khang, Y.H., Khatibzadeh, S., Khoo, J.P., Kok, C., Laden, F., Lalloo, R., Lan, Q., Lathlean, T., Leasher, J.L., Leigh, J., Li, Y., Lin, J.K., Lipshultz, S.E., London, S., Lozano, R., Lu, Y., Mak, J., Malekzadeh, R., Mallinger, L., Marcenes, W., March, L., Marks, R., Martin, R., McGale, P., McGrath, J., Mehta, S., Mensah, G.A., Merriman, T.R., Micha, R., Michaud, C., Mishra, V., Hanafiah, K.M., Mokdad, A.A., Morawska, L., Mozaffarian, D., Murphy, T., Naghavi, M., Neal, B., Nelson, P.K., Nolla, J.M., Norman, R., Olives, C., Omer, S.B., Orchard, J., Osborne, R., Ostro, B., Page, A., Pandey, K.D., Parry, C.D.H., Passmore, E., Patra, J., Pearce, N., Pelizzari, P. M., Petzold, M., Phillips, M.R., Pope, D., Pope, C.A., Powles, J., Rao, M., Razavi, H., Rehfuess, E.A., Rehm, J.T., Ritz, B., Rivara, F.P., Roberts, T., Robinson, C., Rodriguez-Portales, J.A., Romieu, I., Room, R., Rosenfeld, L.C., Roy, A., Rushton, L., Salomon, J.A., Sampson, U., Sanchez-Riera, L., Sanman, E., Sapkota, A., Seedat, S., Shi, P.L., Shield, K., Shivakoti, R., Singh, G.M., Sleet, D.A., Smith, E., Smith, K.R., Stapelberg, N.J.C., Steenland, K., Stockl, H., Stovner, L.J., Straif, K., Straney, L., Thurston, G.D., Tran, J.H., Van Dingenen, R., van Donkelaar, A., Veerman, J.L., Vijayakumar, L., Weintraub, R., Weissman, M.M., White, R.A., Whiteford, H., Wiersma, S.T., Wilkinson, J.D., Williams, H.C., Williams, W., Wilson, N., Woolf, A. D., Yip, P., Zielinski, J.M., Lopez, A.D., Murray, C.J.L., Ezzati, M., 2012. A comparative risk assessment of burden of disease and injury attributable to 67 risk factors and risk factor clusters in 21 regions, 1990-2010: a systematic analysis for the Global Burden of Disease Study 2010. Lancet 380, 2224–2260. https://doi.org/10.1016/S0140-6736(12)61766-8.

Lin, M., Horowitz, L.W., Payton, R., Fiore, A.M., Tonnesen, G., 2017. US surface ozone trends and extremes from 1980 to 2014: quantifying the roles of rising Asian emissions, domestic controls, wildfires, and climate. Atmos. Chem. Phys. 17, 2943–2970. https://doi.org/10.5194/acp-17-2943-2017.

Liu, H., Liu, C., Xie, Z., Li, Y., Huang, X., Wang, S., Xu, J., Xie, P., 2016. A paradox for air pollution controlling in China revealed by "APEC Blue" and "Parade Blue,". Sci. Rep. 6, 34408. https://doi.org/10.1038/srep34408.

Liu, H., Zhang, M., Li, H., Chen, L., 2019. Episode analysis of regional contributions to tropospheric ozone in Beijing using a regional air quality model. Atmos. Environ. 199, 299–312. https://doi.org/10.1016/j.atmosenv.2018.11.044.

Lupaşcu, A., Butler, T., 2019. Source attribution of European surface O3 using a tagged O3 mechanism. Atmos. Chem. Phys. 19, 14535–14558. https://doi.org/10.5194/acp-19-14535-2019.

Mertens, M., Kerkweg, A., Grewe, V., Jöckel, P., Sausen, R., 2020. Attributing ozone and its precursors to land transport emissions in Europe and Germany. Atmos. Chem. Phys. 20, 7843–7873. https://doi.org/10.5194/acp-20-7843-2020.

Monks, S.A., Arnold, S.R., Emmons, L.K., Law, K.S., Turquety, S., Duncan, B.N., Flemming, J., Huijnen, V., Tilmes, S., Langner, J., Mao, J., Long, Y., Thomas, J.L., Steenrod, S.D., Raut, J.C., Wilson, C., Chipperfield, M.P., Diskin, G.S., Weinheimer, A., Schlager, H., Ancellet, G., 2015. Multi-model study of chemical and physical controls on transport of anthropogenic and biomass burning pollution to the Arctic. Atmos. Chem. Phys. 15, 3575–3603. https://doi.org/10.5194/acp-15-3575-2015.

Myhre, G., Shindell, D., Breon, F.-M., Collins, W., Fuglestvedt, J., Huang, J., Koch, D., Lamarque, J.-F., Lee, D., Mendoza, B., Nakajima, T., Robock, A., Stephens, G., Takemura, T., Zhang, H., 2013. Anthropogenic and natural radiative forcing. In: Stocker, T.F., Qin, D., Plattner, G.-K., Tignore, M., Allen, S.K., Boschung, J., Nauels, A., Xia, Y., Bex, V., M. Midgley, P. (Eds.), Climate Change 2013: the Physical Science Basis. Contribution of Working Group I to the Fifth Assessment Report of the Intergovernemental Panel on Cliamte Change. Cambridge University Press, Cambridge, UK and New York, NY, USA.

O'Neill, B.C., Tebaldi, C., van Vuuren, D.P., Eyring, V., Friedlingstein, P., Hurtt, G., Knutti, R., Kriegler, E., Lamarque, J.-F., Lowe, J., Meehl, G.A., Moss, R., Riahi, K., Sanderson, B.M., 2016. The scenario model Intercomparison Project (ScenarioMIP) for CMIP6. Geosci. Model Dev. (GMD) 9, 3461–3482. https://doi.org/10.5194/gmd-9-3461-2016.

Pfister, G.G., Walters, S., Emmons, L.K., Edwards, D.P., Avise, J., 2013. Quantifying the contribution of inflow on surface ozone over California during summer 2008. J. Geophys. Res. Atmos. 118, 12282–12299. https://doi.org/10.1002/2013JD020336.

Price, C., Penner, J., Prather, M., 1997. NO_x from lightning: 1. Global distribution based on lightning physics. J. Geophys. Res. 102, 5929–5941. https://doi.org/10.1029/96JD03504.

Schultz, M.G., Schroder, S., Lyapina, O., Cooper, O.R., Galbally, I., Petropavlovskikh, I., Von Schneidemesser, E., Tanimoto, H., Elshorbany, Y., Naja, M., Seguel, R.J., Dauert, U., Eckhardt, P., Feigenspahn, S., Fiebig, M., Hjellbrekke, A.-G., Hong, Y.-D., Kjeld, P.C., Koide, H., Lear, G., Tarasick, D., Ueno, M., Wallasch, M., Baumgardner, D., Chuang, M.-T., Gillett, R., Lee, M., Molloy, S., Moolla, R., Wang, T., Sharps, K., Adame, J.A., Ancellet, G., Apadula, F., Artaxo, P., Barlasina, M. E., Bogucka, M., Bonasoni, P., Chang, L., Colomb, A., Cuevas-Agullo, E., Cupeiro, M., Degorska, A., Ding, A., Frohlich, M., Frolova, M., Gadhavi, H., Gheusi, F., Gilge, S., Gonzalez, M.Y., Gros, V., Hamad, S.H., Helmig, D., Henriques, D., Hermansen, O., Holla, R., Huber, J., Im, U., Jaffe, D.A., Komala, N., Kubistin, D., Lam, K.-S., Laurila, T., Lee, H., Levy, I., Mazzoleni, C., Mazzoleni, L.R., McClure-Begley, A., Mohamad, M., Murovec, M., Navarro-Comas, M., Nicodim, F., Parrish, D., Read, K. A., Reid, N., Ries, L., Saxena, P., Schwab, J.J., Scorgie, Y., Senik, I., Simmonds, P., Sinha, V., Skorokhod, A.I., Spain, G., Spangl, W., Spoor, R., Springston, S.R., Steer, K., Steinbacher, M., Suharguniyawan, E., Torre, P., Trickl, T., Lin, W., Weller, R., Xu, X., Xue, L., Ma, Z., 2017. Tropospheric ozone assessment Report: database and metrics data of global surface ozone observations. Elem. Sci. Anth. 5, 58. https://doi.org/10.1525/elementa.244.

Shen, J., Zhang, Y., Wang, X., Li, J., Chen, H., Liu, R., Zhong, L., Jiang, M., Yue, D., Chen, D., Lv, W., 2015. An ozone episode over the pearl river delta in October 2008. Atmos. Environ. 122, 852–863. https://doi.org/10.1016/j.atmosenv.2015.03.036.

Shu, L., Wang, T., Han, H., Xie, M., Chen, P., Li, M., Wu, H., 2020. Summertime ozone pollution in the Yangtze River Delta of eastern China during 2013–2017: synoptic impacts and source apportionment. Environ. Pollut. 257, 113631. https://doi.org/10.1016/j.envpol.2019.113631.

Streets, D.G., Fu, J.S., Jang, C.J., Hao, J., He, K., Tang, X., Zhang, Y., Wang, Z., L, Z., Zhang, Q., Wang, L., Wang, B., Yu, C., 2007. Air quality during the 2008 Beijing Olympic games. Atmos. Environ. 41, 480–492. https://doi.org/10.1016/j.atmosenv.2006.08.046.

Stevenson, D., Dentener, F., Schultz, M., Ellingsen, K., Van Noije, T., Wild, O., Zeng, G., Amann, M., Atherton, C., Bell, N., 2006. Multimodel ensemble simulations of present-day and near-future tropospheric ozone. J. Geophys. Res. 111, D08301. https://doi.org/10.1029/2005JD006338.

Stevenson, D.S., Young, P.J., Naik, V., Lamarque, J.-F., Shindell, D.T., Voulgarakis, A., Skeie, R.B., Dalsoren, S.B., Myhre, G., Berntsen, T.K., Folberth, G.A., Rumbold, S.T., Collins, W.J., MacKenzie, I.A., Doherty, R.M., Zeng, G., van Noije, T.P.C., Strunk, A., Bergmann, D., Cameron-Smith, P., Plummer, D.A., Strode, S.A., Horowitz, L., Lee, Y. H., Szopa, S., Sudo, K., Nagashima, T., Josse, B., Cionni, I., Righi, M., Eyring, V., Conley, A., Bowman, K.W., Wild, O., Archibald, A., 2013. Tropospheric ozone changes, radiative forcing and attribution to emissions in the atmospheric chemistry and climate model Intercomparison Project (ACCMIP). Atmos. Chem. Phys. 13, 3063–3085. https://doi.org/10.5194/acp-13-3063-2013.

Sudo, K., Akimoto, H., 2007. Global source attribution of tropospheric ozone: long-range transport from various source regions. J. Geophys. Res. 112, D12302. https://doi.org/10.1029/2006JD007992.

Szopa, S., Naik, V., Adhikary, B., Artaxo, P., Berntsen, T., Collins, W.D., Fuzzi, S., Gallardo, L., Kiendler-Scharr, A., Klimont, Z., Liao, H., Unger, N., Zanis, P., 2021. Short-lived climate forcers. In: Masson-Delmotte, V., Zhai, P., Pirani, A., Connors, S. L., Péan, C., Berger, S., Caud, N., Chen, Y., Goldfarb, L., Gomis, M.I., Huang, M., Leitzell, K., Lonnoy, E., Matthews, J.B.R., Maycock, T.K., Waterfield, T., Yelekçi, O., Yu, R., Zhou, B. (Eds.), Climate Change 2021: the Physical Science Basis. Contribution of Working Group I to the Sixth Assessment Report of the Intergovernmental Panel on Climate Change. Cambridge University Press, Cambridge, United Kingdom and New York, NY, USA, pp. 817–922. https://doi.org/10.1017/9781009157896.008.

Thomas, J.L., Dibb, J.E., Huey, L.G., Liao, J., Tanner, D., Lefer, B., von Glasow, R., Stutz, J., 2012. Modeling chemistry in and above snow at Summit, Greenland – Part 2: impact of snowpack chemistry on the oxidation capacity of the boundary layer. Atmos. Chem. Phys. 12, 6537–6554. https://doi.org/10.5194/acp-12-6537-2012.

Tilmes, S., Lamarque, J.-F., Emmons, L.K., Kinnison, D.E., Ma, P.-L., Liu, X., Ghan, S., Bardeen, C., Arnold, S., Deeter, M., Vitt, F., Ryerson, T., Elkins, J.W., Moore, F., Spackman, J.R., Val Martin, M., 2015. Description and evaluation of tropospheric chemistry and aerosols in the community Earth System model (CESM1.2). Geosci. Model Dev. (GMD) 8, 1395–1426. https://doi.org/10.5194/gmd8-1395-2015.

Turner, M.C., Jerrett, M., Pope, C.A., Krewski, D., Gapstur, S.M., Diver, W.R., Beckerman, B.S., Marshall, J.D., Su, J., Crouse, D.L., Burnett, R.T., 2015. Long-Term ozone exposure and mortality in a large prospective study. Am. J. Resp. Crit. Care 193, 1134–1142. https://doi.org/10.1164/rccm.201508-1633OC.

Val-Martin, M., Heald, C.L., Arnold, S.R., 2014. Coupling dry deposition to vegetation phenology in the Community Earth System Model: implications for the simulation of surface O_3. Geophys. Res. Lett. 41, 2988–2996. https://doi.org/10.1002/2014gl059651.

Van Marle, M.J.E., Kloster, S., Magi, B.I., Marlon, J.R., Daniau, A.-L., Field, R.D., Arneth, A., Forrest, M., Hantson, S., Kehrwald, N.M., Knorr, W., Lasslop, G., Li, F., Mangeon, S., Yue, C., Kaiser, J.W., van der Werf, G.R., 2017. Historic global biomass burning emissions for CMIP6 (BB4CMIP) based on merging satellite observations with proxies and fire models (1750–2015). Geosci. Model Dev. (GMD) 10, 3329–3357. https://doi.org/10.5194/gmd-10-3329-2017.

Voulgarakis, A., Naik, V., Lamarque, J.-F., Shindell, D.T., Young, P.J., Prather, M.J., Wild, O., Field, R.D., Bergmann, D., Cameron-Smith, P., Cionni, I., Collins, W.J., Dalsøren, S.B., Doherty, R.M., Eyring, V., Faluvegi, G., Folberth, G.A., Horowitz, L. W., Josse, B., MacKenzie, I.A., Nagashima, T., Plummer, D.A., Righi, M., Rumbold, S. T., Stevenson, D.S., Strode, S.A., Sudo, K., Szopa, S., Zeng, G., 2013. Analysis of present day and future OH and methane lifetime in the ACCMIP simulations. Atmos. Chem. Phys. 13, 2563–2587. https://doi.org/10.5194/acp-13-2563-2013.

Wang, P., Wang, T., Ying, Q., 2020. Regional source apportionment of summertime ozone and its precursors in the megacities of Beijing and Shanghai using a source-oriented chemical transport model. Atmos. Environ. 224, 117337. https://doi.org/10.1016/j.atmosenv.2020.117337.

Wang, X., Fu, T., Zhang, L., Cao, H., Zhang, Q., Ma, H., Shen, L., Evans, M.J., Ivatt, P.D., Lu, X., Chen, Y., Zhang, L., Feng, X., Yang, X., Zhu, L., Henze, D.K., 2021. Sensitivities of ozone air pollution in the beijing–tianjin– Hebei area to local and upwind precursor emissions using adjoint modeling. Environ. Sci. Technol. 55, 5752–5762. https://doi.org/10.1021/acs.est.1c00131.

Wang, Y., Jiang, S., Huang, L., Lu, G., Kasemesan, M., Yaluk, E., Liu, H., Liao, J., Bian, J., Zhang, K., Chen, H., Li, L., 2023. Differences between VOCs and NOx transport contributions, their impacts on O_3, and implications for O_3 pollution mitigation based on CMAQ simulation over the Yangtze River Delta. China. Sci. Total Environ. 872, 162118. https://doi.org/10.1016/j.scitotenv.2023.162118.

Wang, Z., Li, J., Wang, X., Pochanart, P., Akimoto, H., 2006. Modeling of regional high ozone episode observed at two mountain sites (Mt. Tai and huang) in East China. J. Atmos. Chem. 55, 253–272. https://doi.org/10.1007/s10874-006-9038-6.

Yang, Y., Wang, H., Smith, S.J., Zhang, R., Lou, S., Yu, H., Li, C., Rasch, P.J., 2018. Source apportionments of aerosols and their direct radiative forcing and long-term trends over continental United States. Earths Future 6, 793–808. https://doi.org/10.1029/2018EF000859.

Yao, Y., Wang, W., Ma, K., Tan, H., Zhang, Y., Fang, F., He, C., 2023. Transmission paths and source areas of near-surface ozone pollution in the Yangtze River delta region, China from 2015 to 2021. J. Environ. Manag. 330, 117105. https://doi.org/10.1016/j.jenvman.2022.117105.

Zhang, L., Jacob, D.J., Boersma, K.F., Jaffe, D.A., Olson, J.R., Bowman, K.W., Worden, J. R., Thompson, A.M., Avery, M.A., Cohen, R.C., Dibb, J.E., Flock, F.M., Fuelberg, H. E., Huey, L.G., McMillan, W.W., Singh, H.B., Weinheimer, A.J., 2008. Transpacific transport of ozone pollution and the effect of recent Asian emission increases on air quality in North America: an integrated analysis using satellite, aircraft, ozonesonde, and surface observations. Atmos. Chem. Phys. 8, 6117–6136. https://doi.org/10.5194/acp-8-6117-2008.

Zheng, J., Zhong, L., Wang, T., Louie, P.K.K., Li, Z., 2010. Ground-level ozone in the Pearl River Delta region: analysis of data from a recently established regional air quality monitoring network. Atmos. Environ. 44, 814–823. https://doi.org/10.1016/j.atmosenv.2009.11.032.